

Chapter 7

Aging and saturated repair

We are now ready to build a theory of aging based on the patterns and molecular mechanisms we have seen. Our payoff will be a first-principle explanation of why genetically identical organisms die at different times. We will also understand the origin of the Gompertz law and determine the dynamics of anti-aging interventions.

A theory for aging based on our three laws

To link the dynamics of aging to molecular and cellular mechanisms we present a theory based on our three laws. We will then test it in multiple ways. The theory is agnostic as to the form of damage that is causal for aging, and we will apply it to humans and to other organisms.

To get intuition about the model, let's begin with a story about trucks. A young organism is like a small village where each house produces garbage. The village has 100 garbage trucks, more than enough to clear the garbage. Every year a new house is built, and houses are not removed. With time the village grows; the number of houses rises linearly with time. It eventually becomes a big city that produces a lot of garbage every day. However, this village was not designed to be so large, so there are still only 100 trucks. But now the trucks are overloaded, and garbage piles up in the streets. Any extra garbage stays around for a long time until the overwhelmed trucks get to it. Eventually, when garbage is produced at a rate larger than the maximal capacity of the trucks, garbage piles up higher and higher. The situation becomes incompatible with life.

Let's interpret the story in terms of aging. The garbage is damage causal for aging, which we will call X . To be concrete, for mammals we assume that X is the total number of senescent cells in the body. These senescent cells secrete factors that cause chronic inflammation and reduced regeneration, leading to age-related disease and decline. Later, when we discuss other organisms, X will represent other forms of damage.

The houses in the story are **damage producing units**, DPUs, that generate the damage X . They are produced at a constant rate and slowly accumulate in the body over decades. They make 70-year-olds different from 20 year olds. Since DPUs are made at a constant rate but are irremovable, their number rises linearly with age. Thus, the production rate of X rises linearly with age.

Our candidate for DPUs in mammals is altered stem cells, including both DNA mutations and epigenetic changes, with alterations that do not affect the stem cell but do affect the differentiated

cell it produces. As we saw in chapter 6, the number of altered stem cells rises linearly with age. They produce damaged differentiated cells that become senescent.

Houses, or DPU's, are not removed, but the damage that they create, X , is. It is removed by the trucks, which represent damage-removing processes. For senescent cells, the trucks are NK cells and macrophages. The NK cells detect senescent cells by means of special marker proteins that senescent cells display on their surface. The NK cells attach to the senescent cells and inject toxic proteins to kill them. Mice without functioning NK cells show accelerated aging and large amounts of senescent cells. Other immune cells, including macrophages, also play a role by swallowing up the remains of the killed cells.

But since all biological processes saturate (law 2), so does the removal capacity of senescent cells; the trucks become overwhelmed.

Thus, our model has two features: production of damage that rises linearly with age and saturating removal of damage (Fig 7.1).

This sets up an inevitable catastrophe - when production exceeds maximal removal capacity, the amount of damage X rises sharply.

To get a graphic sense of how damage X grows with age, we can use a rate plot. Removal rate saturates as a function of X , whereas production rate, represented by the colored horizontal lines, is low in young organisms and rises with age. The steady-state point is where the lines cross, as production equals removal. With age, the steady-state X accelerates to higher and higher levels (Fig 7.2) because of the saturating shape of the removal curve. When the production rises above the removal curve, which occurs when age exceeds a critical age, all bets are off. The steady state point shifts to infinity, and X grows indefinitely.

Indeed, with age, senescent cells pile up. They secrete factors that cause inflammation and reduce regeneration - their impact thus extends to the entire body. In order to have such systemic effects, the number of senescent cells does not have to be very large. For example, the entire body is

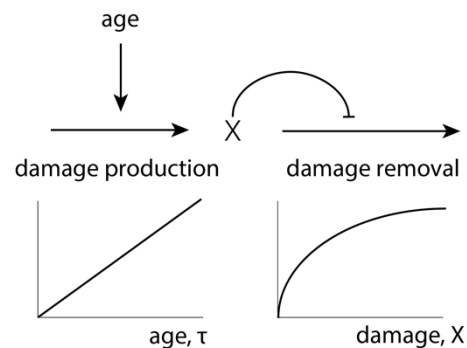


Figure 7.1: The saturating removal model for aging is based on damage that saturates its own removal and whose production rate rises linearly with age.

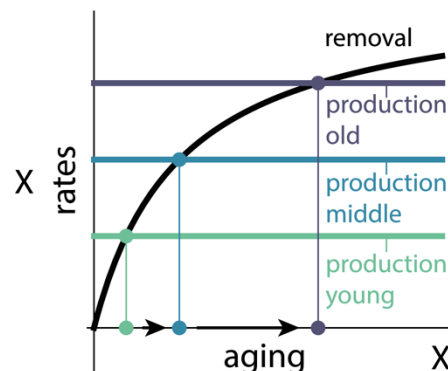


Figure 7.2: A rate plot shows that steady state damage, the point where production and removal curves intersect, accelerates with age.

affected by hormones like cortisol secreted by a 10g gland, which makes up less than 0.1% of the body's cells. Similarly, it may be enough to have only one out of a thousand cells become senescent for their secreted factors to affect physiology at large.

The saturation of the immune cell 'garbage trucks' contributes to decline in another important way: saturation hampers their other tasks, including fighting infection and cancer. Together, these systemic changes increase the risk of illness and organ dysfunction.

Another essential point is the separation of timescales. Just as garbage is made and removed daily, much faster than the rate at which houses are built, so is damage X made and removed much faster than the slow accumulation of damage-producing units. Senescent cell half-life can be days or weeks, whereas their production rate, given by the number of altered stem cells, rises over decades.

Why doesn't the number of trucks rise with age? We can think about this from the point of view of natural selection, in terms of the disposable soma theory. Damage removal capacity, the number of trucks, is selected for the young. The amount of NK cells and macrophages is designed to help young organisms recover from injury. We are not designed to be old - natural selection does not support a mechanism to sufficiently increase removal capacity at old age since most individuals in the wild never reach old age. Indeed, the number of NK cells does not change strongly with age, they just seem more exhausted (Brauning et al. 2022).

More precisely, we can discount as our X any form of damage whose repair mechanism rises with age in a way sufficient to effectively remove X. Damage casual for aging in this theory needs to saturate its trucks when its levels rise sufficiently.

It is likely that each organism has several types of houses, generating several types of garbage, each with its own kind of truck. Perhaps altered stem cells and senescent cells are the first to accumulate; if they were to be eliminated, we might expose the next set of houses and garbage, and so on.

In a nutshell, our theory for aging derives from the three laws:

- All cells come from cells - Stem cells produce differentiated cells.
- Cells mutate - Mutant and epigenetically altered stem-cells increase linearly with age, and they produce damaged and senescent cells.
- Biological processes saturate – the removal processes of these damaged and senescent cells eventually reach their maximal capacity and saturate. Damaged/senescent cell levels rise sharply leading to inflammaging and decline.

Natural selection is the driving force, according to disposable soma theory, because damage removal capacity was selected for the young, not the old, and hence does not increase with age. A useful physiological process in the young, production of senescent cells that cause inflammation as part of normal injury repair, is pushed beyond its specifications to cause inflammaging.

Senescent-cell dynamics in mice can test the model

Our next step is to see what this model predicts for damage, X , namely senescent cell accumulation with age. We would like to compare this to experimental data.

To get a feeling for the dynamics of senescent cells, let's consider an experiment by (Burd et al. 2013) who measured senescent cell abundance in 33 mice every 8 weeks for 80 weeks. To measure whole-body senescent cell amounts, they used genetic engineering to produce mice that emit photons in proportion to the number of senescent cells (Fig 7.3). Photons are produced by a gene from fireflies called **luciferase** that produces light when it acts on a certain substrate. Burd introduced the

luciferase gene into the mouse DNA and placed it under the control of a DNA element, called the p16 promoter, that is primarily activated in senescent cells. Therefore, the senescent cells in these mice make luciferase. When the substrate for luciferase is injected, the mice produce light. Mice normally don't make photons, so the light emitted from the mice provides an estimate of senescent cell abundance, X .

The experiment has several limitations, such as stronger absorption of light from inner regions, some genetic disruption of the natural p16 system which enhanced the chance of cancer so the

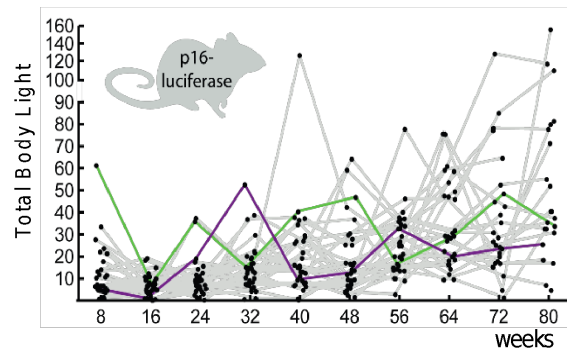


Figure 7.3: Dynamics of a senescent cell reporter in 33 mice over 80 weeks. Light from a p16-luciferase reporter was measured every 8 weeks. Lines connect the data for each individual mouse. Green and purple lines are example trajectories. Adapted from (Burd et al. 2013).

experiment could not probe very old ages, and experimental noise. But the experiment is a good starting point.

Looking at total light emitted from these mice as a measurement of senescent cells X , we see that X rises and falls around an increasing trajectory with age (Fig 7.3). This suggests two timescales: a fast timescale of fluctuations over weeks, and a slow timescale in which X rises over years (Fig 7.4). This fast-slow timescale separation, as mentioned above, is a key element in our model.

Analyzing the data provides five quantitative features to test the theory:

- (i) The *average X grows at an accelerating rate with age* (Fig 7.5 shows the average of the data in Fig 7.3). Such accelerating accumulation with age is also seen in senescent cells in human tissues.
- (ii) The *variation of X between individuals grows with age* (Fig 7.6). Old mice have a larger range of X than young mice. Some old mice even have X levels like young mice (Fig 7.6 shows the standard deviation of the data in Fig 7.3).
- (iii) *Reducing relative heterogeneity*: the standard deviation of X grows more slowly than the mean. Thus, individuals become more similar to each other in relative terms. The standard

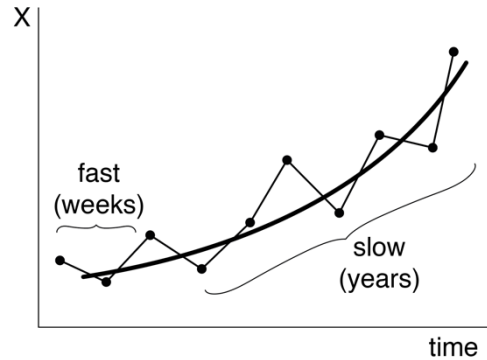


Figure 7.4: Senescent cell data shows separation of timescales, with fast fluctuations over weeks around a slow rise over years.

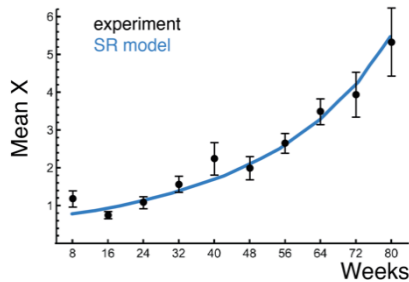


Figure 7.5: Mean level of senescent cells accelerate with age.

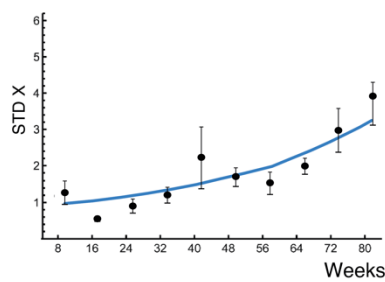


Figure 7.6: Standard deviation of senescent cells rises with age.

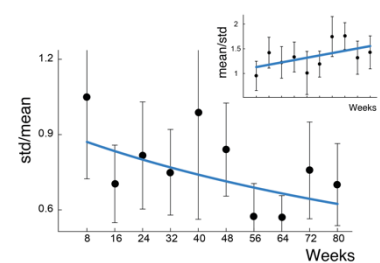


Figure 7.7: Coefficient of variation, defined as $CV = \text{std}/\text{mean}$, of senescent cells drops with age. Inset: $1/CV$ rises with age.

deviation/mean, called the coefficient of variation (CV), drops with age (Fig 7.7); its inverse $1/CV$ rises approximately linearly with age (Fig 7.7 inset).

The declining heterogeneity means that damage X becomes *more similar between individuals with age*. Such similarity might be expected for a core driver of aging. By

contrast, downstream effects of X, like age-related diseases, depend on genetics and environment and are thus more variable between individuals with age.

- (iv) Distributions of X between individuals at a given age are skewed to the right. There are more individuals above average X than below it (Fig 7.8). The skewness of these distributions gradually drops with age, as they become more symmetric.

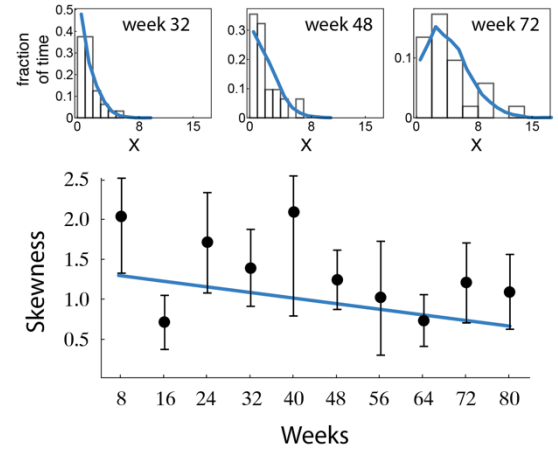


Figure 7.8: Damage distributions are skewed to the right and skewness drops with age.

- (v) The correlation time of X increases with age (Fig 7.9 right). A mouse that is higher or lower than average stays so for longer periods the older it is (Fig 7.9 left panels). Thus, with age, the stochastic variation in X becomes more persistent.

Interestingly, these dynamical features are shared with the human frailty index described in the previous chapter. The mean and standard deviation of frailty rise with age, but relative heterogeneity drops with age, as does the skewness of the frailty distributions. In the next chapter, we will see that senescent cell dynamics are tightly linked with the diseases and conditions that make up the frailty index.

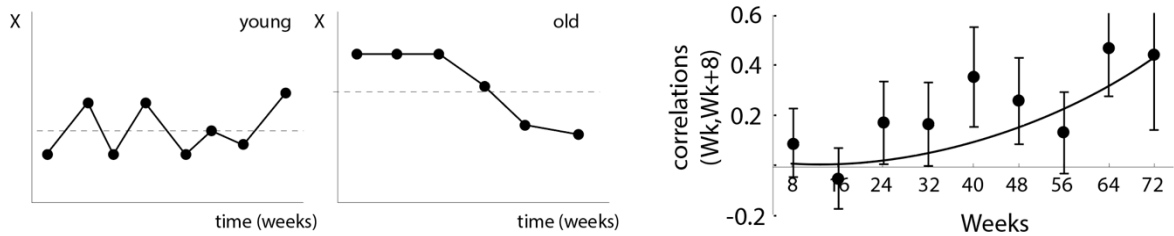


Figure 7.9: Damage fluctuates rapidly in young and becomes more persistent with age as seen in rising correlation time.

The saturating removal model can explain senescent cell dynamics

These dynamical features of senescent cells can be explained by our simple truck model for aging, which we call the **saturating removal** model, as discovered by Omer Karin in his PhD with me. Omer scanned a wide class of models and found that the essential features that a model needs to explain the senescent cell dynamics are precisely the truck model. In fact, these dynamical features are enough to constrain the possible minimal models into a single candidate.

The first feature is **two timescales**, one fast and one slow: X is produced and removed on a timescale that is much faster than the rise in DPU which occurs on the timescale of the lifespan. This separation of timescales allows us to write an equation for the rate of change of X in which the production and removal rates vary slowly and depend on age, τ . The model also includes stochastic noise. Thus,

$$\frac{dX}{dt} = \text{production} - \text{removal} + \text{noise}$$

The production rate of X rises linearly with age in the model:

$$\text{production} = \eta\tau$$

where we use τ for age and t for time to make sure that we understand that there are two timescales: a fast scale (days-weeks) in which damage reaches steady-state, and a slow timescale (years) over which production rate $\eta\tau$ changes.

The removal of X is carried out by removal processes, namely NK cells that kill senescent cells. If this removal worked at a constant rate β per senescent cell, the removal term would thus be $-\beta X$. However, this does not match the data. The equation is $\frac{dX}{dt} = \eta\tau - \beta X$, whose steady-state solution is a linear rise of X with age, $X_{st} = \eta\tau/\beta$. This is ruled out by the data which shows an accelerating rise with age (Fig. 7.5).

Instead, the model explains the accelerating rise in X by a **removal rate that drops with the number of senescent cells**. In other words, removal saturates; senescent cells inhibit their own removal. Such a drop could be due to several processes: immune cells that remove senescent cells could be downregulated if they kill too often, or they can become inhibited by factors that the senescent cells secrete. The drop of removal rate can also be simply due to a saturation effect, in which the removing cells become increasingly outnumbered by senescent cells as senescent cell numbers rise.

To model the saturation, we use a Michaelis-Menten form which is good both for inhibition due to secreted factors and for saturation (see solved exercise 7.3)

$$removal = \beta \frac{X}{\kappa + X}$$

Where β is the maximal senescent-cell removal capacity, in units of senescent cells/time, and κ is the concentration of X at which they inhibit half of their own removal rate. The removal rate *per senescent cell* thus drops with senescent cells abundance, $\frac{\beta}{\kappa + X}$ (Fig 7.10), and the number of senescent cells lost per unit time is that rate times X , namely $\frac{\beta X}{\kappa + X}$.

Combining production and removal, we obtain a model for the rate of change of X :

$$\frac{dX}{dt} = \eta\tau - \beta \frac{X}{\kappa + X} \quad [1]$$

Note that this model assumes that maximal removal capacity β does not decline with age. Adding such a decline, namely $\beta(\tau)$, generally leaves the conclusions the same. For simplicity we ignore this possibility and recall that NK cell numbers do not appreciably drop with age in humans.

Let's compute the steady state of X . On the fast timescale of weeks, the production rate $\eta\tau$ can be considered as constant. Setting $dX/dt = 0$ in Eq. 1 we find that the (quasi-) steady-state X of is

$$X_{st} \approx \frac{\kappa\eta\tau}{\beta - \eta\tau} [2]$$

Thus, X_{st} rises linearly with age at first. Then, the term on the bottom becomes closer and closer to zero, which is a critical point. The rise of X accelerates and diverges at a critical age $\tau_c = \beta/\eta$ (Fig 7.11). Fig 7.4 shows a good agreement between data in dots and the model in black.

When X levels rise high enough, they reach levels not compatible with life. Thus, the critical age $\tau_c = \beta/\eta$ is a rough approximation for the mean lifespan. This equation indicates that lifespan can be extended by increasing the repair capacity β , or by reducing the senescent-cell production rate η . More trucks or slower construction of houses.

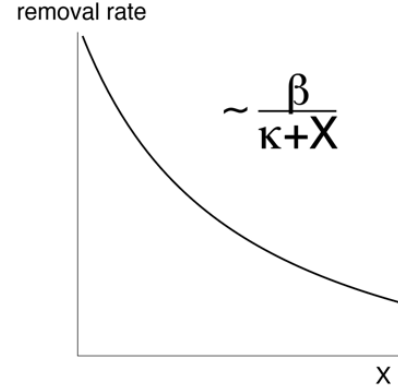


Figure 7.10: Removal rate per senescent cell drops with senescent cell abundance X .

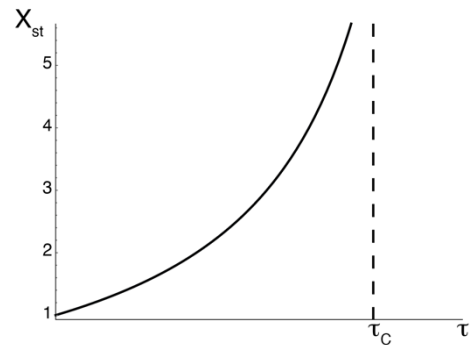


Figure 7.11: Mean senescent cells X accelerates and diverges at a critical age.

Adding noise to the model explains the variation between individuals in senescent-cell levels

If this model was all there was, then all individuals would age at the same rate and die at the same age. In other words, so far, the model does not explain why genetically identical organisms differ in the number of senescent cells. We need to describe the fluctuations of X over time which produce the differences between individuals. To understand these stochastic features of the dynamics, we need to add **noise** to the model.

The simplest way to add noise is to add a white-noise term ξ . This white noise term adds and removes small amounts of X randomly, with mean zero and a variance described by the parameter 2ϵ . The factor 2 is for convenience in the equations below. The noise describes fluctuations in production and removal due to internal or external reasons such as injury, infection, and stress (cortisol). In fact, we don't currently know what the noise describes. White noise is a convenient way to wrap up our ignorance in a mathematical object that we can work with.

We arrive at the main model of this chapter and the next, a stochastic differential equation called the **saturating removal model**:

$$\frac{dX}{dt} = \eta\tau - \beta \frac{X}{X + \kappa} + \sqrt{2\epsilon}\xi \quad [3]$$

Let's take a nice deep sigh of relief to celebrate making it to this point.

The saturating removal model captures the variation between individuals

We will now use this model to understand the dynamics of senescent cells, and then to understand the origin of the Gompertz law. Let's begin with the variation in X between individuals at a given age. To do so, we need to compute the damage distribution, $P(X)$.

There is an elegant way to compute the damage distribution. Historically, this approach comes from analysis of particles undergoing Brownian motion under the influence of forces, known in physics as Langevin equations. I like this approach because it has a graphic interpretation in which X is the position of a particle rolling down a bowl-shaped contour (Fig 7.12). To describe the bowl, one recasts equation 3 using a potential function $U(X)$. The potential function is the shape of the bowl. The slope of the potential provides the restoring force that pushes the particle back to the equilibrium at the bottom of the bowl: the slope $-dU/dX$ is defined as production minus removal,

$-dU/dx = \eta\tau - \beta \frac{X}{X+\kappa}$. At the bottom of the bowl the slope is zero, and thus production equals removal, so that the bottom is the position of the steady state.

The required potential is $U(X) = (\beta - \eta\tau)X - \beta\kappa \log(\kappa + X)$. You can check this by taking the derivative $-dU/dX$ to verify that it gives $\eta\tau - \beta \frac{X}{X+\kappa}$.

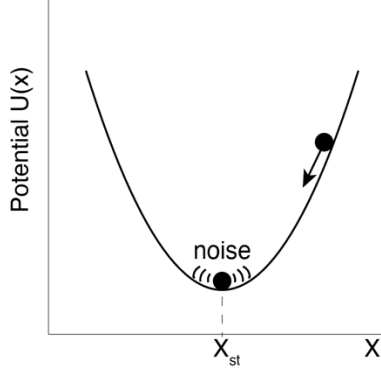


Figure 7.12: Damage dynamics can be likened to a particle in a bowl-shaped potential well jiggled by noise.

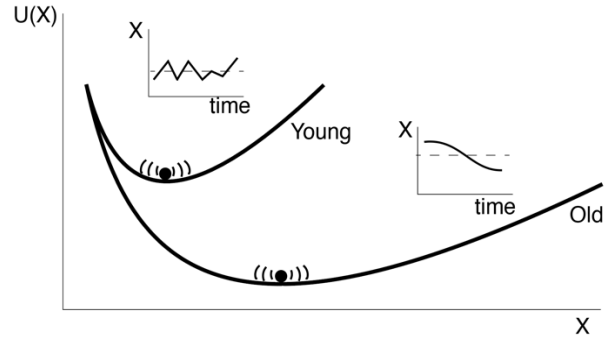


Figure 7.13: With age the bowl widens to the right, increasing damage mean and variance.

The particle rolls down to the bottom of the bowl and noise randomizes its position (Fig 7.12). The distribution of X that we seek is then analogous to the Boltzmann law that applies to particles in a potential under thermal fluctuations. The noise amplitude ϵ plays the role of temperature, and we obtain $P(X) \sim e^{-U/\epsilon}$. The mathematical details are provided in solved exercise 7.1 at the end of the chapter.

In essence, at young ages the senescent cells are like a particle in a steep potential well because removal is not saturated and pushes hard on senescent cells towards low levels. The particle is jiggled by noise in the narrow well, and so $P(X)$ is narrowly distributed around a low mean damage (Fig 7.13). With age, the potential well opens to the right, as production rate rises, and the mean damage increases and so does its variance (Fig 7.13).

The saturating removal model thus predicts a distribution of damage that we can find by plugging in the potential into the Boltzmann term $P(X) \sim e^{-U/\epsilon}$ to obtain

$$P(X) \propto e^{-\frac{(\beta - \eta\tau)X}{\epsilon}} (\kappa + X)^{\frac{\beta\kappa}{\epsilon}} \quad [6]$$

This distribution rises with X , reaches a peak, and then falls exponentially. It is skewed to the right, and matches the skewed distributions observed in the mouse data (Fig 7.8, upper panel, blue lines). This distribution provides an improved estimate for the average X that takes noise into account,

$$\langle X \rangle \approx \frac{\kappa\eta\tau + \epsilon}{\beta - \eta\tau} \quad [7]$$

The mean X rises with age and diverges at age $\tau_c = \frac{\beta}{\eta}$. The standard deviation of X also rises with age and diverges at τ_c :

$$\sigma \approx \frac{\sqrt{\kappa\beta + \epsilon^2}}{\beta - \eta\tau} \quad [8]$$

This rise in the mean and standard deviation matches the observed rise with age of the standard-deviation of the light emitted from the mice of Burd et al (Burd et al. 2013) (Fig 7.5 and 7.6, blue lines).

Notably, the model even captures the fact that variation rises more slowly than the mean – the phenomenon of reducing relative heterogeneity. The ratio between the standard deviation and the mean of X , the coefficient of variation CV , drops with age as observed

$$CV = \frac{\sigma}{\langle X \rangle} \approx \frac{\sqrt{\kappa\beta + \epsilon^2}}{\kappa\eta\tau + \epsilon} \sim 1/\tau.$$

This reducing heterogeneity is a distinguishing feature of the model. Most simple stochastic models show a constant CV .

The model also captures the increasing correlation times with age. At young ages, the bowl is steep. Thus, if X is away from steady-state X_{st} , it returns to it quickly (Fig 7.13). At old age, in contrast, the bowl is almost completely flat. The trajectory of the particle is dominated by noise, with little restoring force coming from the steepness of the bowl (Fig 7.13). Hence individuals that stray away from X_{st} have a weak restoring force and stay away for longer times.

Such increasing correlation times have a general name in physics, “**critical slowing down**”. They are a mark of an approaching phase transition. In the canonical example of a phase transition, the boiling of water, large and slow fluctuations in density can be seen near the boiling point. In other areas of science, slowing down of fluctuations can be a warning sign of a big transition. Examples include climate fluctuations before an ice age, or ecological fluctuations before a species extinction [Schaffer 2009]. In our case, the phase transition is to infinite X , which is death.

The mouse data allows estimating the four model parameters, η, β, κ and ϵ . The best fit parameters are approximately $\eta = 4 \cdot 10^{-4} \text{ days}^{-2} \sim 0.15/\text{year}/\text{day}$, $\beta = 0.3/\text{day}$, $\kappa = 1$, $\epsilon = 0.1$, in units where the average senescent cells level in young mice is 1. The rough estimate of lifespan $\tau_c = \frac{\beta}{\eta} \sim 2 \text{ years}$ is about right for mice.

These parameters give a specific prediction for the half-life of a senescent cell. The half-life is about 5 days in young mice and rises to about a month in old mice (25 days in 22-month old mice)

because the trucks are overloaded. These predictions were intriguing enough to test experimentally, which Omer Karin did with senescent-cell expert Valery Krizhanovsky. In young mice the senescent cell half-life was 5 ± 1 days. In old mice (22-month-old), removal was much slower, with an estimated half-life of about a month. These measurements agree well with the predictions of the model.

Gompertz mortality with slowdown is found in the model

We can now finally ask why do genetically identical organisms die at different times? What explains the exponential increase in risk of death with age (the Gompertz law), and the deceleration of risk at very old ages (Fig 7.14)?

To connect senescent-cell dynamics to mortality, we need to know the relationship between senescent cell abundance and the risk of death. The precise relationship is currently unknown. Let's therefore simply model death when senescent-cell abundance exceeds a threshold level X_c (Figure 7.15). The threshold represents a collapse of an organ system or a tipping point such as sepsis. Thus, death is a **first-passage time process**, when senescent cells cross X_c .

We use this threshold-crossing assumption to illustrate a way of thinking, because it provides analytically solvable results. Other dependencies between risk of death and senescent cell abundance, such as Hill functions with various degrees of steepness, provide similar conclusions.

Again, there is an elegant way to solve this first passage time problem and obtain the risk of death as a function of age. To estimate the probability that X crosses the death-threshold X_c , we apply an approach which is analogous to the rate of a chemical reaction crossing an energy barrier ΔG , namely the Boltzmann factor, $e^{-\frac{\Delta G}{k_b T}}$. In our case the noise amplitude ϵ plays the role of temperature $k_b T$, and the energy barrier is the difference between the potential U at X_c and at the

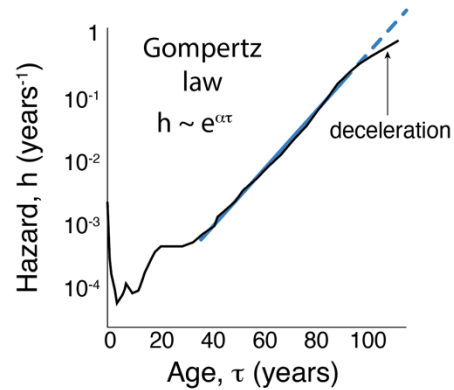


Figure 7.14: The risk of death rises exponentially according to the Gompertz law and decelerates at very old ages.

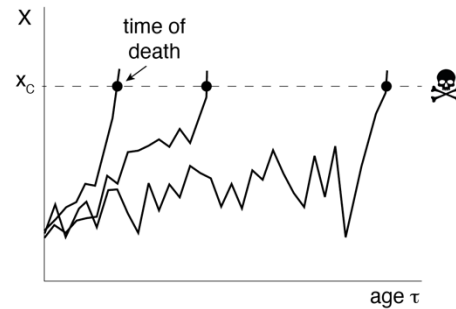


Figure 7.15: Death is modelled to occur when X crosses a threshold X_c .

steady-state value X_{st} , $\Delta U = U(X_c) - U(X_{st})$. Thus, the probability per unit time for X crossing X_c , namely the risk of death that we call the hazard, is

$$h \approx e^{-\frac{\Delta U}{\epsilon}}$$

This equation is called Kramer's equation in the field of stochastic processes. An intuitive explanation is that the particle in the well needs to climb a potential difference of $\Delta U = U(X_c) - U(X_{st})$ to fall off into the death region (Fig 7.16). It needs to climb using 'kicks' provided by the

noise of size ϵ . Each noise kick can be either to the right or left. Since you need $\frac{\Delta U}{\epsilon}$ kicks, all in the right direction, the chance is exponentially small and goes as $e^{-\frac{\Delta U}{\epsilon}}$ (Fig. 7.17).

Now because the production rate of senescent cells rises

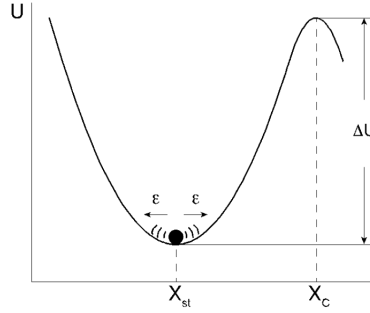


Figure 7.16: The particle needs to climb a potential difference of with noise kicks of size in order to fall off into the death region

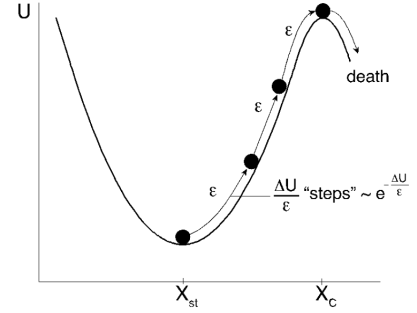


Figure 7.17: Death requires kicks in the same direction whose chance is exponentially small.

linearly with age, it becomes easier and easier to reach the threshold X_c . As the potential bowl opens up, the 'energy barrier' drops linearly with age, and risk therefore rises exponentially with age. The outcome for the risk of death (see solved exercise 7.1) is, upto age-independent factors:

$$h(\tau) \approx (\beta - \eta\tau)^{\frac{\kappa\beta}{\epsilon}+1} e^{\frac{(\kappa+X_c)\eta\tau}{\epsilon}} \quad [9]$$

This is a big moment. The hazard rises exponentially with age as $e^{\alpha\tau}$ with an exponent α , called the **Gompertz aging rate**, given by

$$\alpha = \frac{(\kappa+X_c)\eta}{\epsilon}.$$

The Gompertz aging rate can thus be written in terms of molecular parameters: noise, damage production rate and death thresholds. The aging rate is proportional to the slope of damage production with age, η . It is inversely proportional to the noise amplitude ϵ . Aging rate also rises with the death threshold X_c (see solved exercise 7.1 for further discussion).

The Gompertz law is thus intimately related to the linear rise with age of the production rate. If the production rate rose with age not linearly $\eta\tau$ but as age squared, for example, $\eta\tau^2$, we would not get the Gompertz law but instead a hazard that rises exponentially with age squared, $e^{\alpha\tau^2}$.

This solution also explains the observed deceleration of the hazard rate at very old ages (when $\eta\tau \approx \beta$). This deceleration is due to the prefactor $(\beta - \eta\tau)^{\frac{\kappa\beta}{\epsilon}+1}$ which becomes small as age

approaches the critical age $\tau_c = \beta/\eta$. Fundamentally, slowdown occurs because near the critical age production and removal rates are nearly equal and cancel out, and noise becomes the primary driver of X . Therefore, damage dynamics resemble a random walk, with a nearly constant probability per unit time of crossing the threshold¹.

The saturating removal model thus analytically reproduces the Gompertz law, including the deceleration of mortality rates at old ages (Fig 7.18). It gives a good fit to the observed mouse mortality curve using parameters that agree with the experimental half-life measurements and longitudinal senescent cells data. The inferred threshold for death is $X_c = 17 \pm 2$, meaning that the threshold X_c is about 17 times larger than the mean senescent-cell level in young individuals.

Thus, genetically identical mice die at different times due to noise amplified by accumulating damage producing units and a saturating damage removal.

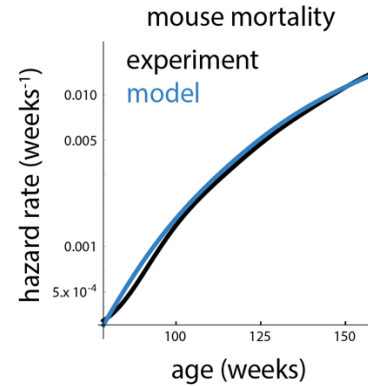


Figure 7.18: The saturating removal model analytically captures the Gompertz law and deceleration of mortality in mice.

The human Gompertz law is captured as well

So far, we calibrated the model on mouse data. Let's now use it to study human mortality curves. In humans, as in mice, mortality has a large non-heritable component estimated at 80% of the variation in lifespan.

We can ask which of the model parameters changes between mice and humans to provide the difference in their lifespans. A good description of human hazard curves, corrected for extrinsic mortality, is provided by the same parameters as in mice, except for a 60-fold slower increase in η , the slope of senescent-cell production with age. Figure 7.19 shows the model with added extrinsic mortality at a level indicated by the dashed line, in comparison to the observed mortality.

¹ Note that the analytical approximation begins to be inaccurate when $\eta t > \beta$, and simulations of the full model are needed to compute the hazard curve at old ages. Simulations show that the rise of the hazard curve slows and converges to a constant hazard at very old ages.

The smaller value of η in humans can be due to improved DNA maintenance and enhanced damage repair in humans compared to mice. Thus, there are fewer DPUs at a given age, and each DPU gives rise to fewer senescent cells. Fewer houses each making less garbage.

Indeed, studies that compare mammalian species show that rates of DNA mutation, epigenetic alteration and translation errors are all inverse to lifespan in different mammals (Figure 7.20) (Cagan et al. 2022; Ake Lu et al. 2021).

The theory therefore suggests that the parameter η is the main knob that evolution tunes in order to generate the lifespans of different mammals, as in the mass-longevity triangle of the previous chapter.

What practical use does the theory have? We end this chapter with ways in which the saturating removal model conceptualizes approaches to slow down aging. As we show in the next chapter, the model can address the use of drugs that eliminate senescent cells, known as senolytic drugs (Kirkland and Tchkonja 2020) (Zhang et al., 2022). It provides the strength and frequency of treatment needed to reduce age-related diseases and addresses the question of whether starting treatment at old age can be effective. Stay tuned.

The saturating removal model explains aging patterns also in organisms that lack senescent cells

The theory makes specific predictions, making it a falsifiable theory. If it fails to explain an experimental pattern, we throw it out. That is why we like to test the model against as many patterns as possible. To do so, we turn to a wider range of organisms.

It is remarkable that diverse organisms show the Gompertz law and the other patterns of aging we saw in the previous chapter. Even single-celled organisms show the Gompertz law under

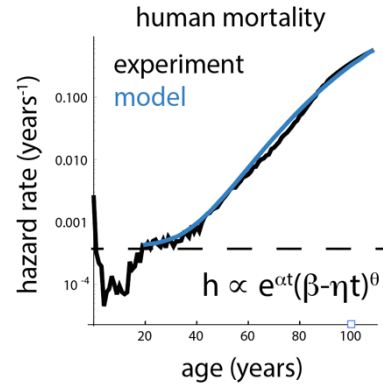


Figure 7.19: The saturating removal model with additive constant extrinsic mortality reproduces the Gompertz law and deceleration of mortality in humans.

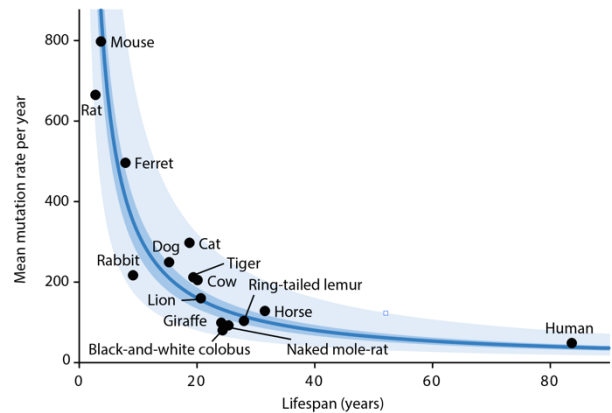


Figure 7.20: Mutation rate per stem cell is inversely proportional to lifespan in mammals. Adapted from (Cagan et al 2022).

certain conditions. Examples include starved *E. coli* cells (Yang et al. 2019) and yeast cells with asymmetric replication called budding (Steinkraus, Kaerberlein, and Kennedy 2008).

These model organisms lack senescent cells, but all show the nearly universal features of aging shared with mice and humans. To understand this, recall that the model is agnostic about the molecular nature of the damage X and the damage producing units. It can therefore be generalized beyond senescent cells. It should apply to any form of damage that is causal for aging as long as it has saturating-removal-type dynamics, namely turnover that is much faster than the lifetime, production rate that rises linearly with age and saturating removal.

We therefore compare the model to key experiments in organisms without senescent cells such as yeast, the fruit fly *Drosophila melanogaster* and the roundworm *C. elegans*.

Let's think of how the saturating removal model can apply to single-celled organisms or simple animals. We need a DPU, a factor that accumulates in cells with time and is irremovable, and which generates damage X . Surveying the massive experimental research on model organisms shows recurring themes which can serve as candidate DPUs. One of these candidates is aggregates of unfolded proteins which the cell is unable to remove. These aggregates grow inside the cell and cause damage such as mitochondrial damage and reactive oxygen species (Labbadia and Morimoto 2015).

Let's use protein aggregates as an example. The mass of the aggregates, $P(t)$, grows when misfolded proteins join the aggregate. Since the cell makes proteins at a constant rate, and each protein has a chance to be misfolded due to transcription/translation errors, P grows at a constant rate, $dP/dt = a$, and thus $P = a t$. Indeed, older single celled organisms have larger aggregates.

The aggregates P are toxic to cells. They produce damage X , whatever its exact nature, at rate b per unit aggregate. Damage production is thus $bP = a b t$. We can therefore define the parameter η as $\eta = a b$. According to law 2, the removal mechanisms of the damage X saturate, and we have the saturating removal model, $dX/dt = \eta t - \beta X/(\kappa + X) + noise$.

Other molecular factors can play the role of the DPUs, such as rDNA circles in yeast caused by epigenetic alterations. We conclude that the model can be plausible also for single-celled model organisms, and more generally to invertebrates that lack senescent cells.

Rapid shifts between hazard curves

As we saw in the previous chapter, shifting fruit flies to a life-extending diet led to a rapid switch to the better survival curve within a couple of days. The sins of the past are forgiven (Fig 6.12). In contrast, shifting temperature only changed the slope of the death curve, and the accumulated past hazard was not forgotten (Fig 6.13).

These phenomena can be explained by the saturating removal model based on the rapid turnover of damage X and the irremovable nature of damage producing units.² The plummet to a

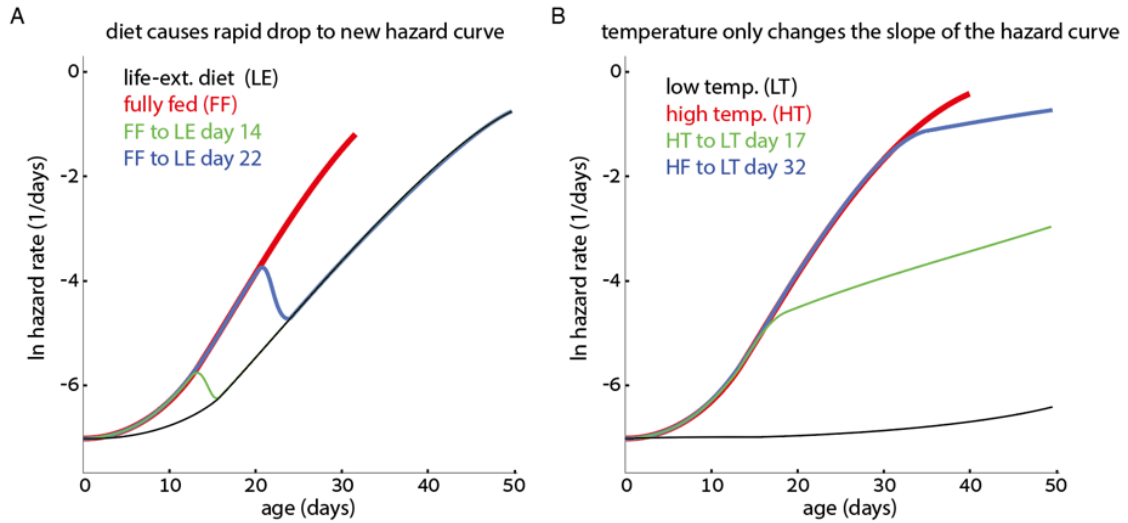


Figure 7.21: Saturating removal model captures the rapid shift to the better hazard curve when diet is changed to a lifespan-extending diet, and the change of hazard slope upon a shift to lower growth temperature.

lower curve after a shift of diet in Fig 7.21A can be explained if the diet lowers the amount of damage produced by each damage-producing unit, P . The life-extending diet shifts the tradeoff from growth to repair, so that each P makes less damage X per unit time, namely a lower value of the parameter b . It's as if the denizens of the houses begin to conserve, reuse and recycle and thus produce less garbage.

Therefore, after the shift, the production term $\eta t = aP(t)$ is lower, and the hazard curve shifts down. The time it takes to move between curves is the rapid turnover time of the damage X , on the order of hours to days in flies. When recycling begins, the trucks clear the garbage rapidly. The model predicts that this 'transient' time should grow with age due to slowdown of removal.

In contrast, the slope change of hazard induced by temperature in Fig 7.21B can be explained by a reduced rate of production of new damage producing units- slower construction of new houses. This a reduction in the accumulation parameter a in the equation $dP/dt = a$, without a change in b , the rate of damage production per unit P . Thus, P keeps its accumulated number but is produced more slowly starting from the temperature shift at time t_0 . Thus, $P(t) = a t_0 + a' (t - t_0)$, where a' is the reduced production rate. This results in the hazard curve shown in Fig 7.21B.

² A parameter set for flies is $\beta=1 \text{ hr}^{-1}$, $\epsilon=1 \text{ hr}^{-1}$ and $\eta=0.03 \text{ hr}^{-1} \text{ day}^{-1}$, $XC=15$. Flies on a life-extending diet have a lower production slope $\eta=0.02 \text{ hr}^{-1} \text{ day}^{-1}$.

Scaling of survival curves

A further test is whether the model can explain the **scaling** of survival curves for *C. elegans*, yeast and mice under different life-extending or life-shortening genetic, environmental and diet perturbations. Recall that scaling means that the survival curves collapse on the same curve when age is scaled by mean lifespan. Few things get physicists more excited than a good data collapse, where different curves fall on top of each other when normalized. Such a collapse reveals that perturbations that are superficially unrelated to each other actually impact the system in the same way.

Most interventions that increase lifespan also show scaling. For example, caloric restriction shows survival curves that collapse nearly onto the same curve when age is normalized by median lifespan (Fig 7.22). Scaling seems to apply in all organisms tested for caloric restriction.

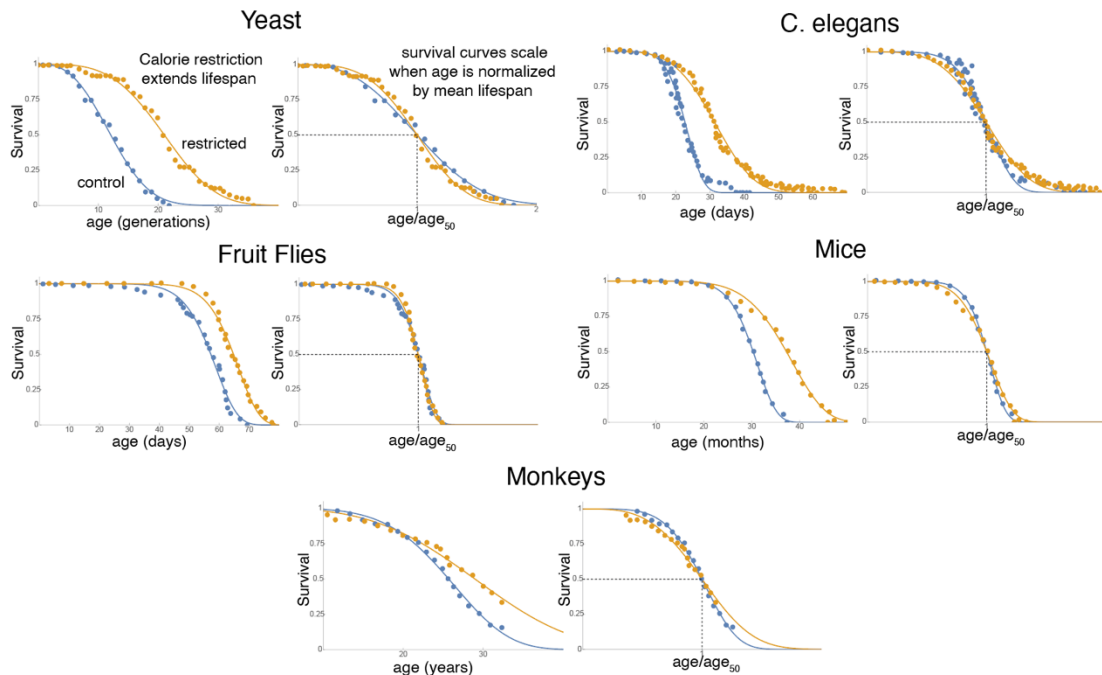


Figure 7.22: Caloric restriction increases lifespan with scaling of survival curves in different species. Adapted from (Conn's Handbook of Models for Human Aging (Second Edition) Chapter 19)

The model provides this scaling property to an excellent approximation, for perturbations that affect the production rate parameter η (Figure 7.23 A). Lowering the damage production rate η lengthens lifespan but preserves the shape of the survival curve.

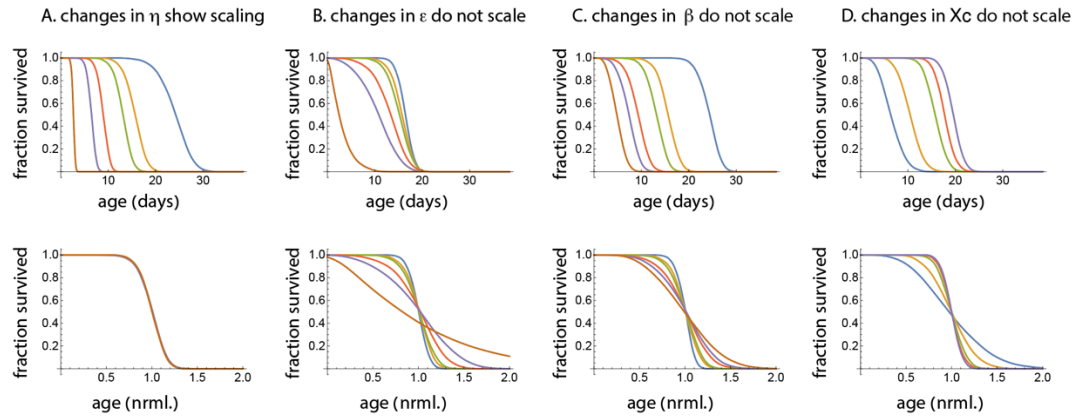


Figure 7.23: Scaling is found in the saturating removal model upon changes in damage production slope, but not changes in other parameters, the removal rate, noise or death threshold X_c .

Caloric restriction is indeed thought to reduce the rate of damage production by slowing down the ‘rate of living’ so that there is less metabolic activity, and shifting the cells into increased repair and recycling, as mentioned above. This should reduce the rate of DPU production and toxicity per DPU, reducing η .

The pathways for the effects of caloric restriction include the IGF1 pathway mentioned in chapter 6. Lifespan extension by mutations in this pathway, such as *daf-2* mutations in worms, were among the first life-span-extending mutations found, as you can read in the history by pioneer aging researcher Cynthia Kenyon (Kenyon 2011). These mutations shift the entire survival curve to longer lifetimes but maintain its shape showing scaling (Fig 7.24). Similar longevity and scaling is seen in IGF1 mutations across organisms.

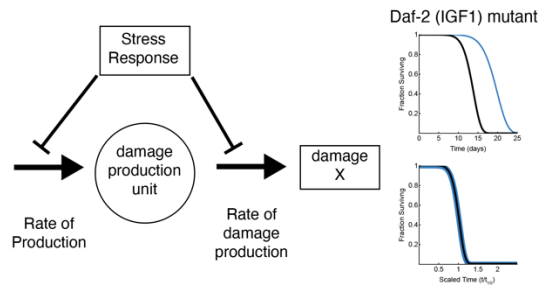


Figure 7.24: Inhibiting the IGF1 pathway affects production of damage, increasing lifespan with survival-curve scaling.

Interestingly, there is no scaling in the model when a perturbation affects other parameters, such as removal rate β (Fig 7.23 C). Thus, there is no scaling when the trucks are affected. When removal rate β is increased, the model predicts that lifespan increases and the survival curve becomes steeper. The reason for the steeper curve is that damage has a shorter half-life due to faster removal, and thus there is less time for noise to randomize things. Survival becomes more deterministic, and organisms die at more similar times.

Since scaling is so common in yeast, worms, and mice, we may conclude that many perturbations affect damage production rate, η , but very few affect the removal trucks. Finding mutations or interventions that do not scale will help to pinpoint the identity of the trucks and garbage in each organism. This prediction may apply to exceptional perturbations in which scaling is not found such as the *nuo-6* mutation in worms that affects mitochondrial repair.

One prediction is that removing senescent cells by senolytic drugs should make mice not only live longer but make their survival curves steeper. This is because senolytic drugs increase the removal rate β of senescent cells. Steeper survival curves are indeed found in studies on senolytic drugs as shown in Fig 7.25 .

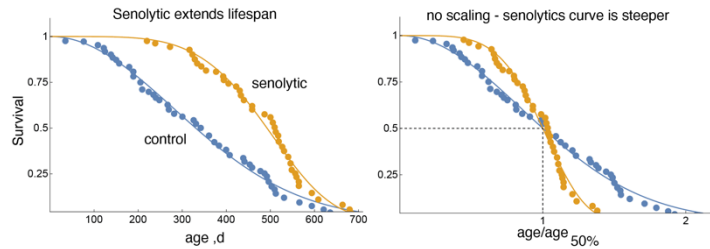


Figure 7.25: Senolytic drugs increase mean mice lifespan and show steepened survival curves as predicted by model. Adapted from (adapted from Kowald and Kirkwood 2021).

Another intervention in mice that increases lifespan and steepens the survival curve is inhibiting the age-associated loss of blood vessels. Inducing growth of blood vessels by mild overexpression of the vascular regulator VEGF (Grunewald et al. 2021) caused a nearly 40% increase in mouse lifespan (Fig 7.26), with reduced senescent cell load, delayed cancer and improved organ function. Increased blood vessels have many positive effects including better oxygen flow to organs. One of the effects of increased blood vessels is more roads for the trucks- access for the immune cells that remove senescent cells, thus potentially increasing their removal rate β and explaining the steeper survival curves.

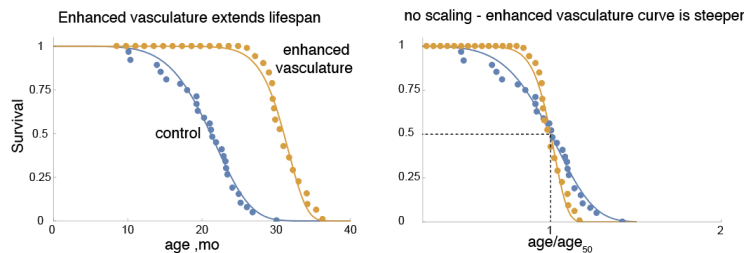


Figure 7.26: Enhanced vasculature in mice increases mean lifespan and shows steepened survival curves. Adapted from (Grunewald et al. 2021)

Approaches to slow down aging and aging-related diseases

Current medicine focuses on treating each age-related disease one at a time: diabetes, cancer, heart disease and so on. A different approach would be to deal with their shared risk factor - to slow the aging process, or more precisely to slow the rise of senescent cells and other aging-related damage. This is the **Geroscience hypothesis**: *slowing the core process of aging will prevent and mitigate multiple age-related diseases in one fell swoop.*

The conceptual framework we discussed points to two general strategies: reduce production rate η or increase removal capacity β .

Reducing production can be achieved by boosting cellular damage-repair systems (Fig. 7.27). One way to achieve this is caloric restriction and other types of restricted feeding. As mentioned above, fasting shifts the balance from growth towards maintenance in cells. Effort is devoted to developing drugs that mimic caloric restriction by, for example, perturbing the IGF1 pathway; these drugs include mTOR inhibitors. One promising drug is metformin, used for treating diabetes since the 1920s. Metformin inhibits the IGF1 pathway, and seems to tip the balance towards more repair. An encouraging sign is that people taking metformin have lower risk of cancer. A current effort is to convince the federal food and drug administration (FDA) to allow clinical trials for aging; currently only trials for a specific disease are allowed. Metformin is one suggested drug for such a trial, along with other mTOR inhibitors such as rapamycin.

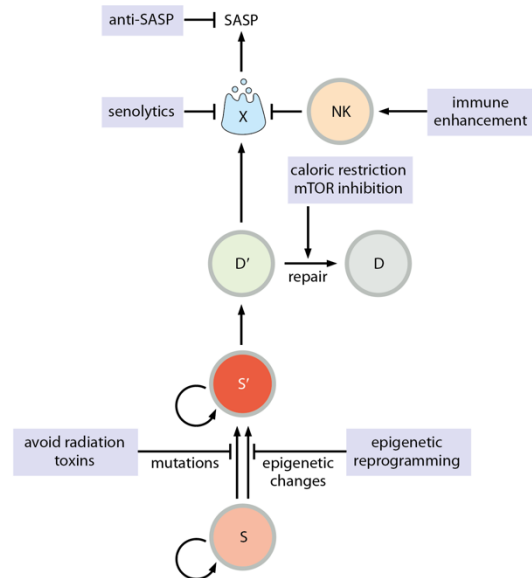


Figure 7.27: Approaches to slow down aging target damage production and removal processes.

Increasing the removal rate of senescent cells is also an attractive possibility. That is what **senolytic drugs** do. Senolytics remove senescent cells by exploiting the Achilles heels of senescent cells that are not found in most other cells. One such drug, for example, inhibits an anti-cell-death pathway called bcl2, exploiting the fact that this pathway helps senescent cells resist death to a greater extent than most other cells in the body. There are several additional families of senolytics. Some are entering clinical trials in humans for specific diseases (Zhang et al., 2022).

The number of garbage trucks and hence the maximal removal capacity β can also be increased by immune-based strategies. Recently, an immune approach used to fight cancer cells was repurposed to remove senescent cells in mice (Amor et al. 2020). In this approach, called CAR-T, killer T-cells are taken from the mouse and genetically engineered to express a receptor that recognizes a protein found only on the surface of senescent cells. These engineered T-cells were reintroduced into the mice and killed senescent cells. Another potential approach targets the factors that senescent cells secrete, such as pro-inflammatory factors, and reduces their effect.

It would be elegant to reduce production at its root, the DPUs, by targeting the altered stem cells, but this is challenging. Approaches that mitigate epigenetic changes, such as cell

reprogramming or drugs that modulate enzymes that add or remove epigenetic marks have shown promise in certain aging contexts (Eisenstein 2022). Some of the reprogramming approaches currently face unwanted side effects, however, because they revert cells to primordial stem-like states that increase the risk of cancer.

Non-pharmacological approaches that offer a degree of rejuvenation have been known for ages. These are the quartet of exercise, healthy diet, good sleep and reduced stress by means of social relationships, purposeful action, psychotherapy, meditation and moderation. Exercise has coordinated beneficial effects including lowering insulin resistance and reducing excess fat in tissues. Healthy diet likewise reduces fat and insulin spikes. Easing the mind reduces stress including the activity of the HPA axis and sympathetic nervous system. This positively impacts insulin resistance and blood pressure and may enhance the maintenance roles of the immune system.

A sobering note for hopes of immortality. Even if one removes senescent cells, mice still eventually get sick and die. For example, mutant and altered stem cells produce damaged cells in all tissues. Many of these damaged cells do not become senescent but still have reduced function and cause inflammatory responses. As damaged cells increase in number they will eventually cause an organ system to fail. As mentioned above, there is likely a series of causal factors, and removing one reveals the next like peeling an onion. There is probably a brain-specific factor related to Alzheimer's disease. Damaged neurons accumulate with age and set off neuroinflammation, raising the specter of prevalent dementia at ages above 90 as the price of increased longevity due to amelioration of cancer and heart disease.

Furthermore, with age, organs like the skin, gut and lung are increasingly composed of small local 'kingdoms' of cells, each from a different clone of stem cells. Each clone arises from an altered stem cell that has a growth advantage relative to its neighbors. Each kingdom thus has its own individual random mutations. In people above 70, for example, most blood cells are made from a few stem-cell clones in the bone marrow (Mitchell et al. 2022). Blood health depends on the luck of which mutations these stem cells have. Thus, although senescent cells are a major component, other factors are likely to be important for aging.

In this intense chapter we described a theory of aging. It explains why genetically identical organisms die at different times, and why risk of death rises exponentially with age, why survival curves scale and other universal patterns of aging. The theory consists of biological processes with wide generality: linearly rising damage production and saturating removal. It can thus apply to senescent cells in humans and also to other forms of damage in

invertebrates without senescent cells. The theory explains how different perturbations alter survival curves and conceptualizes ways to extend healthspan.

Speaking of healthspan, the next chapter will explore age-related diseases.

Exercises:

Solved exercise 7.1: compute the distribution of damage X at a given age in the saturating removal model

The distribution of X , denoted $P(X)$, is the probability of having X senescent cells.

To calculate the distribution $P(X)$, we use a method that applies to any stochastic differential equation of the form: $\frac{dX}{dt} = v(X) + \sqrt{2\epsilon}\xi$. In the model, the ‘velocity’ $v(x)$ equals production minus removal, namely $v(X) = \eta\tau - \beta X/(\kappa + X)$. The idea is to rewrite the equation using a **potential** $U(X)$, whose slope is determined by the velocity as follows: $\frac{dU}{dX} = -v(X)$.

The potential function has the shape of a bowl (Fig 7.14). The variable X is like a ball rolling in the bowl (Fig 7.14). The ball rolls down the slope, with velocity $-v(x)$ given by the slope of the bowl, dU/dX . The steeper the bowl, the faster the ball rolls. The bowl can be considered to be coated with a thick goo, as described in Strogatz’s superb book on dynamical systems (Strogatz 2001), and so the ball slogs through the goo in a damped way and settles down at the minimum of the bowl without oscillating. At the minimum point the slope is zero, $dU/dX = 0$, and that is where the steady state is, $X = X_{st}$. The steeper the sides of bowl, the faster the ball returns to X_{st} when it is perturbed.

Let’s now add noise. Noise jiggles the ball position X so that it deviates from X_{st} . These jiggles cause a distribution of X values, $P(X)$. Again, the steeper the bowl, the less noise can move X away from X_{st} , and the narrower the distribution $P(X)$.

The nice thing about the potential-function way of writing the equation is that we can easily compute the steady-state distribution. This distribution $P(X)$ for a given age t is given by the Boltzmann distribution, with ϵ playing the role of temperature:

$$P(X) \propto e^{-\frac{U(X)}{\epsilon}} \quad [5]$$

An intuitive explanation is provided in solved exercise 7.3. The shallower the bowl, or the larger the ‘temperature’, the wider the distribution $P(X)$.

For the saturating removal model, the potential $U(X)$ is

$$U(X) = (\beta - \eta\tau)X - \beta\kappa \log(\kappa + X) \quad [6]$$

We can safely assume that age τ is constant over the fast timescale needed to reach the steady-state distribution $P(X)$, except at very old ages. Plotting $U(X)$ shows that at young ages the bowl is steep, and therefore the distribution is localized around the mean (Fig 7.28). With age, the bowl

becomes more and more shallow, because its right-hand slope drops as $-\eta\tau$. At the critical age, when $\eta\tau = \beta$, the bowl opens up and the mean X at steady state goes to infinity.

Plugging $U(X)$ from Eq. 6 into the Boltzmann-like law of Eq 5 we obtain the distribution

$$P(X) \propto e^{-\frac{(\beta-\eta\tau)X}{\epsilon}} (\kappa + X)^{\frac{\beta\kappa}{\epsilon}} \quad [6]$$

which reaches a peak and then falls

exponentially with X . This distribution of senescent cells in the model is skewed to the right, consistent with the skewed distributions observed in the mouse data (Fig 7.10, blue lines). With age, the skewness of this distribution drops (Fig 7.11 blue line).

Solved exercise 7.2: Show that the saturating removal model gives the Gompertz law of mortality.

To estimate the probability that X crosses the death-threshold X_c , we apply Kramers law

$$h \approx e^{-\frac{U(X_c) - U(X_{ST})}{\epsilon}}$$

The potential U in our model is given by Eq.3. For the Gompertz law to hold, one needs the term $\frac{U(X_c) - U(X_{ST})}{\epsilon}$ to decrease linearly with age τ , so that $h \approx e^{a\tau}$.

The exponent of the hazard rate in the model indeed shows the required linearity in time. This is the factor $\eta\tau$ in this complicated expression:

$$-\frac{U(X_c) - U(X_{ST})}{\epsilon} = \frac{(\kappa + X_c)\eta\tau - X_c\beta + \kappa\beta \cdot \text{Log} \left[\frac{(\kappa + X_c)(\beta - \eta\tau)}{\kappa\beta} \right]}{\epsilon} \quad [8]$$

Which can be written, up to a prefactor that does not depend on age, as:

$$h(\tau) \approx e^{-\frac{\beta X_c}{\epsilon}} (\beta - \eta\tau)^{\frac{\kappa\beta}{\epsilon} + 1} e^{\frac{(\kappa + X_c)\eta\tau}{\epsilon}} \quad [9]$$

The prefactor $e^{-\frac{\beta X_c}{\epsilon}}$ indicates that the hazard at age zero drops exponentially with the threshold X_c . Thus, although X_c increases the logarithmic slope of the hazard $\alpha = \frac{(\kappa + X_c)\eta\tau}{\epsilon}$, the intercept at age zero drops exponentially with X_c . Thus hazard at a given age is overall reduced by increasing the threshold X_c . This makes sense since a higher threshold makes it more difficult for X to cross X_c .

Solved exercise 7.3: Intuitive derivation of the Boltzmann-like form of the steady-state distribution:

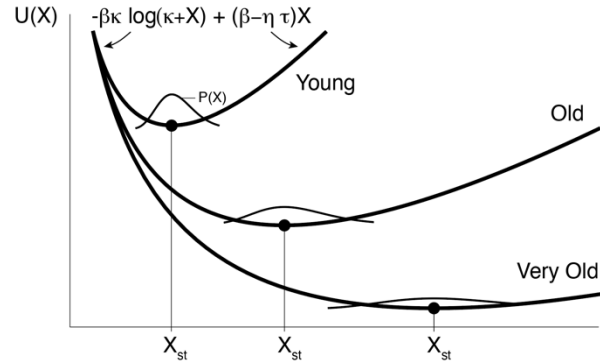


Figure 7.28: Potential in the saturating removal model widens to the right with age.

Consider a stochastic process of the form $\frac{dX}{dt} = v(x) + \sqrt{2\epsilon}\xi$. The function $v(x)$ is called the velocity of x . In the model, we have a velocity equal to production minus removal: $v(x) = \eta t - \frac{\beta x}{\kappa + x}$. Define the potential $U(x)$ by $\frac{dU}{dx} = -v(x)$. Explain intuitively why, at steady-state, the probability distribution is $P(x) = P_0 \exp\left(-\frac{U(x)}{\epsilon}\right)$.

Solution: Consider a large number of particles moving along a one-dimensional pipe. They diffuse with diffusion coefficient ϵ and are also swept along the pipe by a velocity field $v(x)$. The particle density at steady-state is $P(x)$. The flux at point x due to the velocity field is the velocity times the density: $v(x)P(x)$. The flux due to diffusion can be found by Fick's law of diffusion, which shows a diffusive flux from high to low densities proportional to the gradient: $-\epsilon dP/dx$. At steady-state total flux is zero, so that the two fluxes must sum to zero: $v(x)P - \epsilon dP/dx = 0$. Thus, $\frac{dP}{dx} = \frac{v(x)P(x)}{\epsilon}$. The solution is $P(x) = P_0 \exp\left(-\frac{U(x)}{\epsilon}\right)$. Thus, at steady-state, in regions where velocity is large the density $P(x)$ shows a steep opposing slope so that diffusion flux can balance velocity flux.

7.4 Survival and hazard functions:

- (a) Show that hazard, $h(\tau)$, defined as the probability of death per unit time, is related to survival $S(\tau)$ as follows

$$h(\tau) = -\frac{1}{S} \frac{dS(\tau)}{d\tau} = -\frac{d \log S(\tau)}{d\tau}$$

- (b) Show that $S(\tau) = e^{-\int h(\tau) d\tau}$
- (c) What is the survival function S when the hazard follows the Gompertz-law? Plot this survival function.
- (d) What is the survival function if hazard is constant $h(\tau) = h_0$?
- (e) A tree has a hazard function that drops with age, $h(\tau) = \frac{a}{1+b\tau}$. What is the survival function? Plot and compare to d and c. What might be a biological cause of such a decreasing hazard function?

7.4 Removal of Senescent cells based on saturating their own removal process: Senescent cells are removed by immune cells such as NK cells, which we will denote by R . There are a total of R_T removing cells in the body, and that this number does not change appreciably with age (as is indeed the case for NK cells in humans). The R cells meet Senescent cells, denoted X , at rate k_{on} to form

a complex $[R X]$ which can either fall apart at rate k_{off} , or end up killing the Senescent cells at rate v . Thus, $R + X \rightleftharpoons [RX] \rightarrow R$.

(a) Explain the following dynamic equation for the complex:

$$\frac{d[RX]}{dt} = k_{on} R X - (v + k_{off})[RX]$$

(b) Use the fact that R cells can be either free or in a complex, so that $R + [RX] = R_T$, to show that the removal rate of Senescent cells is

$$removal = \frac{\beta X}{k + X}$$

(c) What are the values of the maximal removal capacity β , and the half-way saturation point k ? Explain intuitively.

a. No repair: Consider an accumulation process of damage with constant production and no removal

$$\frac{dX}{dt} = \eta + \sqrt{2\epsilon}\xi .$$

7 What is the mean damage X as a function of age?

8 What is the distribution $P(X)$?

9 What is the hazard assuming that death occurs when $X > X_c$? Is there a Gompertz law?

7.6 Age-dependent reduction in repair capacity: Consider a process in which damage is produced at a constant rate η , and removal does not saturate. Removal rate per cell drops with age,

$$\frac{dX}{dt} = \eta + (\beta - \beta_1 \tau)X + \sqrt{2\epsilon}\xi .$$

(a) What is the mean damage X ?

(b) What is the distribution $P(X)$ at age ?

(c) What is the ratio of mean and standard deviation of X : $\langle X \rangle / \sigma$?

(d) What is the hazard, if death occurs when $X > X_c$? Is there a Gompertz law?

7.7 Deterministic model: Assume that the Gompertz law arises not from stochastic effects, but instead from individual differences, set a birth, in X production and removal parameters, in which each individual i has its own noise-free equation $\frac{dX}{dt} = \eta_i - \beta_i X$. Death is modeled to occur when X crosses threshold X_c . What distribution of production and removal parameters η_i, β_i can provide the Gompertz law? What features does this model not explain?

7.8 Parameter effects: What is the effect on the hazard curve of the saturating removal model of a change in each of the parameters $\beta, \eta, \epsilon, \kappa$? Plot examples of hazard curves to demonstrate your answer.

7.9 Senescent cell half-life: show that in the saturating removal model, the half-life of a senescent cell is

$$t_{1/2} = \log(2)(\kappa\beta + \epsilon)/\beta(\beta - \epsilon\tau)$$

7.10 Critical slowing down: Read (Scheffer et al. 2009).

7 How does critical slowing down relate to the model?

8 Suggest a phenomenon beyond those discussed in Scheffer which might show critical slowing down and suggest an experiment or measurement to test this.

7.11 (Challenging question) General model: Damage is produced at rate $\eta(X, \tau)$ and removed at rate $\beta(X, \tau)$. The equation is $\frac{dX}{dt} = \eta(X, \tau) - \beta(X, \tau) + \sqrt{2\epsilon}\xi$

(a) What is the steady-state distribution at age τ ?

(b) What is the risk of death as a function of age, modeled by first passage time of a threshold X_c ?

(c) Under which conditions does risk of death go as the Gompertz law?

7.12 Strehler and Mildvan (1960) model for the Gompertz law. Strehler and Mildvan (STREHLER and MILDVAN 1960) (SM) proposed a phenomenological process for the Gompertz law. Organisms are assumed to start with an initial survival capacity, termed V , declining linearly with age x as $V(x) = V_0(1 - Bx)$, where B indicates the fraction of vitality loss per unit time. Over life, animals experience random external challenges or insults with a mean frequency K . Challenges have random magnitudes, exponentially distributed with an average magnitude D that expresses the average deleteriousness of the environment. Death occurs when the magnitude of a challenge exceeds the remaining vitality. A review of the SM theory can be found in (Finkelstein 2012).

- Show that these assumptions produce the Gompertz law $h(\tau) = ae^{b\tau}$. Calculate a and b .
- What similarities and differences does this theory have with the model?

7.13 Heterochronic Parabiosis: Parabiosis is the surgical joining of two mice so that they share circulation. When joining a young and an old mouse, known as heterochronic parabiosis, the

young mouse shows signs of aging whereas the old mouse rejuvenates. Senescent cells decrease in the old mouse, whereas they increase in the young mouse.

- (a) Explain these effects using the model. Hint: the trucks from the young mouse can help the old mouse.
- (b) The survival curve of the old mouse is made steeper and that of the young mouse less steep compared to a control experiment joining two equal-aged mice. Explain using the model.
- (c) Develop an extended model that describes heterochronic parabiosis. Assume that senescent cells stay in the tissues and are not shared by the mice, but that the immune cells that remove them are shared through the circulation. Plot senescent cells in each of the two mice as a function of time after joining. See (Karin and Alon 2021).

7.14 **Aging rates of different organs.** Based on the model, would you expect that different organs in the same individual will age at similar rates or different rates? Explain (100 words).

SR model	$\dot{X} = \eta t - \frac{\beta X}{X + \kappa} + \sqrt{2\epsilon}\xi$
Mean	$\mu \approx \frac{\kappa\eta t + \epsilon}{\beta - \eta t}$
Standard deviation	$\sigma \approx \frac{\sqrt{\kappa\beta\epsilon + \epsilon^2}}{\beta - \eta t}$
Half-life	$T_{1/2} \approx \frac{\log 2(\epsilon + \kappa\beta)}{\beta(\beta - \eta t)}$

Figure 7.27

- Ake Lu, Viviana Perez, Zhe Fei, Ken Raj, and Steve Horvath. 2021. "Universal DNA Methylation Age Across Mammalian Tissues." *Innovation in Aging* 5 (Supplement_1): 410. <https://doi.org/10.1093/geroni/igab046.1588>.
- Amor, Corina, Judith Feucht, Josef Leibold, Yu-Jui Ho, Changyu Zhu, Direna Alonso-Curbelo, Jorge Mansilla-Soto, et al. 2020. "Senolytic CAR T Cells Reverse Senescence-Associated Pathologies." *Nature* 583 (7814): 127–32. <https://doi.org/10.1038/s41586-020-2403-9>.
- Brauning, Ashley, Michael Rae, Gina Zhu, Elena Fulton, Tesfahun Dessale Admasu, Alexandra Stolzing, and Amit Sharma. 2022. "Aging of the Immune System: Focus on Natural Killer Cells Phenotype and Functions." *Cells* 11 (6): 1017. <https://doi.org/10.3390/cells11061017>.
- Burd, Christin E., Jessica A. Sorrentino, Kelly S. Clark, David B. Darr, Janakiraman Krishnamurthy, Allison M. Deal, Nabeel Bardeesy, Diego H. Castrillon, David H. Beach, and Norman E. Sharpless. 2013. "Monitoring Tumorigenesis and Senescence in Vivo with a P16 INK4a-Luciferase Model." *Cell* 152 (1–2): 340–51. <https://doi.org/10.1016/j.cell.2012.12.010>.
- Cagan, Alex, Adrian Baez-Ortega, Natalia Brzozowska, Federico Abascal, Tim H. H. Coorens, Mathijs A. Sanders, Andrew R. J. Lawson, et al. 2022. "Somatic Mutation Rates Scale with Lifespan across Mammals." *Nature* 604 (7906): 517–24. <https://doi.org/10.1038/s41586-022-04618-z>.
- Eisenstein, Michael. 2022. "Rejuvenation by Controlled Reprogramming Is the Latest Gambit in Anti-Aging." *Nature Biotechnology* 40 (2): 144–46. <https://doi.org/10.1038/d41587-022-00002-4>.
- Finkelstein, Maxim. 2012. "Discussing the Strehler-Mildvan Model of Mortality." *Demographic Research*. <https://doi.org/10.4054/DemRes.2012.26.9>.
- Grunewald, M., S. Kumar, H. Sharife, E. Volinsky, A. Gileles-Hillel, T. Licht, A. Permyakova, et al. 2021. "Counteracting Age-Related VEGF Signaling Insufficiency Promotes Healthy Aging and Extends Life Span." *Science* 373 (6554): eabc8479. <https://doi.org/10.1126/science.abc8479>.
- Karin, Omer, and Uri Alon. 2021. "Senescent Cell Accumulation Mechanisms Inferred from Parabiosis." *GeroScience* 43 (1): 329–41. <https://doi.org/10.1007/s11357-020-00286-x>.
- Kenyon, Cynthia. 2011. "The First Long-Lived Mutants: Discovery of the Insulin/IGF-1 Pathway for Ageing." *Philosophical Transactions of the Royal Society B: Biological Sciences* 366 (1561): 9–16. <https://doi.org/10.1098/rstb.2010.0276>.
- Kirkland, J. L., and T. Tchkonja. 2020. "Senolytic Drugs: From Discovery to Translation." *Journal of Internal Medicine* 288 (5): 518–36. <https://doi.org/10.1111/joim.13141>.
- Labbadia, Johnathan, and Richard I. Morimoto. 2015. "The Biology of Proteostasis in Aging and Disease." *Annual Review of Biochemistry* 84: 435–64. <https://doi.org/10.1146/annurev-biochem-060614-033955>.
- Steinkraus, K.A., M. Kaeberlein, and B.K. Kennedy. 2008. "Replicative Aging in Yeast." *Annual Review of Cell and Developmental Biology* 24: 29–54. <https://doi.org/10.1146/annurev.cellbio.23.090506.123509>.
- STREHLER, B. L., and A. S. MILDVAN. 1960. "General Theory of Mortality and Aging." *Science* 132 (3418): 14–21. <https://doi.org/10.1126/science.132.3418.14>.
- Yang, Yifan, Ana L. Santos, Luping Xu, Chantal Lotton, François Taddei, and Ariel B. Lindner. 2019. "Temporal Scaling of Aging as an Adaptive Strategy of Escherichia Coli." *Science Advances*. <https://doi.org/10.1126/sciadv.aaw2069>.

References

Saturating removal model (Karin et al. 2019)

Saturating removal model and parabiosis (Karin and Alon 2021)

Scaling of survival functions

(Liu and Acar 2018)

Geroscience hypothesis (Austad 2016)

(Furman et al. 2019)

(Gasek et al. 2021)

Review on model organism aging

(Cagan et al. 2022)

Blood clonality in old: (Salminen 2021a) (Salminen 2021b)

Additional Reference:

(Mair et al. 2003)

(Weindruch and Sohal 1997)

(Unnikrishnan et al. 2018)

<https://www.ncbi.nlm.nih.gov/pmc/articles/PMC9337830/>